Ambient measurements of biological aerosol particles near Killarney, Ireland: a comparison between real-time fluorescence and microscopy techniques

D. A. Healy[1#*], J. A. Huffman[2, 3*], D. J. O'Connor[1], C. Pöhlker[3], U. Pöschl[3] and J. R. Sodeau[1]

[1]University College Cork, Department of Chemistry and Environmental Research Institute, Cork, Ireland

[2]University of Denver, Department of Chemistry and Biochemistry, Denver, Colorado, USA

[3]Max Planck Institute for Chemistry, Multiphase Chemistry and Biogeochemistry Departments, Mainz, Germany

[#]Now at Pepsico, Global Quality Services, Cork, Ireland.

*Corresponding authors: d.healy@ucc.ie; alex.huffman@du.edu

Abstract

Primary biological aerosol particles (PBAP) can contribute significantly to the coarse particle burden in many environments. PBAP can thus influence climate and precipitation systems as cloud nuclei and can spread disease to humans, animals, and plants. Measurement data and techniques for PBAP in natural environments at high time- and size- resolution are, however, sparse and so large uncertainties remain in the role that biological particles play in the Earth system. In this study two commercial real-time fluorescence particle sensors and a Sporewatch single-stage particle impactor were operated continuously from 2 August to 2 September 2010 at a rural sampling location in Killarney National Park in south western Ireland. A cascade impactor was operated periodically to collect size-resolved particles during exemplary periods. Here we report the first ambient comparison of the waveband integrated bioaerosol sensor (WIBS-4) with the ultraviolet aerodynamic particle sizer (UV-APS) and also compare these real-time fluorescence techniques with results of fluorescence and optical microscopy of impacted samples. Both real-time instruments showed qualitatively similar behaviour, with increased fluorescent bioparticle concentrations at night when relative humidity was highest and temperature was lowest.

The fluorescent particle number from the FL3 channel of the WIBS-4 and from the UV-APS were strongly correlated and dominated by a 3 µm mode in the particle size distribution. The WIBS FL2 channel exhibited particle modes at approx. 1 and 3 µm, and each were correlated with the concentration of fungal spores commonly observed in air samples collected at the site (ascospores, basidiospores, *Ganoderma spp.*). The WIBS FL1 channel exhibited variable multi-modal distributions turning into a broad featureless single mode after averaging and exhibited poor correlation with fungal spore concentrations, which may be due to the detection of bacterial and non-biological fluorescent particles. *Cladosporium spp.*, which are among the most abundant fungal spores in many terrestrial environments, were not correlated with any of the real-time fluorescence channels, suggesting that the real-time fluorescence instruments are relatively insensitive to PBAP classes with dark, highly absorptive cell walls.

Fluorescence microscopy images of cascade impactor plates showed large numbers of coarse mode particles consistent with the morphology and weak fluorescence

51 expected of sea salt. Some of these particles were attached to biological cells,
52 suggesting that a marine source influenced the PBAP observed at the site and that the
53 ocean may be an important contributor to PBAP loadings in coastal environments.

1. Introduction

The *in situ* monitoring of primary biological aerosol particles (PBAPs) with high time resolution represents an important technological development made capable, in part, by long-standing, military-led research into the detection of biological warfare agents. The more recent drive to monitor ambient, atmospheric PBAPs is largely related to adverse effects they play in human and agricultural health (*e.g.* allergic rhinitis, food crop damage) (Lacey and Dutkiewicz, 1994; Patel and Bush, 2000; Pöschl, 2005; Shiraiwa et al., 2012). Several classes of bioaerosols have been shown to act as cloud and ice nuclei in laboratory settings (e.g. Maki et al., 1974; Diehl et al., 2001; Morris et al., 2004; Möhler et al., 2007; Pummer et al., 2012; Haga et al., 2013; Morris et al., 2013), and ambient measurements have shown PBAP to be ubiquitously associated with rain and snowfall as well as present in clouds (Christner et al., 2008; Pöschl et al., 2010; DeLeon-Rodriguez et al., 2013; Huffman et al., 2013; Prenni et al., 2013). Thus, it has been suggested that PBAP may impact precipitation and the hydrological cycle, and may ultimately affect the weather and climate of a region (Sands et al., 1982; Morris et al., 2008; 2014). A review of biological aerosol properties and detection methods is beyond the scope of this text, but comprehensive PBAP overviews are available (e.g. Madelin, 1994; Ho, 2002; Fröhlich-Nowoisky et al., 2009; Womack et al., 2010; Caruana, 2011; Xu et al., 2011; Després et al., 2012; Fröhlich-Nowoisky et al., 2012).

Common usage of the term PBAP includes various classes of biological particles, including: viruses; bacteria; fungal, moss and fern spores; pollen; algal and plant cells; insects, mites, and their fragments including excreta (Després et al., 2012). Such PBAPs have been well studied within the aerobiology community for many decades using traditional methods of impact collection followed by microscopic counting and identification procedures. These analyses can be time consuming and require significant processing cost and skill. In contrast, relatively few studies have reported ambient collection and analysis of bioaerosols at high time resolution (e.g. seconds to minutes), due to the lack of instrumentation capable of monitoring particles on such fast timescales. Recent studies utilizing real-time PBAP measurements have collected and analysed ambient PBAP data for periods as long as 18 consecutive months (Pan et al., 2007; Huffman et al., 2010; Gabey et al., 2011; Schumacher et al., 2013; Toprak and Schnaiter, 2013). Such measurements obtained with high-time resolution can

subsequently aid our understanding of atmospheric PBAP properties including sub-diurnal boundary layer transport and cloud formation. Recently, work to model bioaerosol emissions on global and regional scales have attempted to quantify the impact that PBAP have on coarse aerosol loadings and ice nuclei properties (e.g. Burrows et al., 2009a; 2009b; Heald and Spracklen, 2009; Hoose et al., 2010; Sesartic et al., 2013; Hummel et al., 2014), however more detailed understanding of PBAP inputs are necessary to constrain model results.

A number of optical systems utilizing light/laser-induced fluorescence (LIF) have been developed to detect airborne biological material based on the presence of biological fluorophores in the particle. Instrumentation available for military research use, but not commercial/civilian use, include: the Aerosol Fluorescence Spectrum Analyser (AFSA) (Pinnick et al., 1995; Pinnick et al., 2004; Pan et al., 2011) and the Single Particle Fluorescence Analyser (SPFA) (Eversole et al., 1999; Sivaprakasam et al., 2011). Within approximately the last decade, commercially available devices have become obtainable for purchase and use by non-military communities. Similar to approaches developed in military-based laboratories, these commercial instruments provide real-time (on-line) detection of biological particles suspended in the air. Two single particle fluorescence instruments that have been used most widely within the atmospheric aerosol research community include the ultraviolet aerodynamic particle sizer (UV-APS; TSI, Inc. model 3314, St. Paul, MN) (Hairston et al., 1997; Brosseau et al., 2000; Huffman et al., 2010) and the waveband integrated bioaerosol sensor (WIBS; originally developed by the University of Hertfordshire, UK and now licensed and sold by Droplet Measurement Technology, Boulder, CO) (Kaye et al., 2005; Foot et al., 2008; Stanley et al., 2011). Fluorescent emission excited by ~360 nm radiation is considered to include the presence of metabolites (e.g. NAD(P)H, riboflavin) within living cells. Emission related to excitation by ~280 nm radiation is usually attributed to proteins and amino acids present in all biological material, whether living or dead (Pöhlker et al., 2012; 2013). However observed fluorescence signals at a given wavelength are likely to arise from a complex mixture of bio-fluorophores in the particle (Pöhlker et al., 2012).

A growing body of published reports suggest that particle autofluorescence can be used, to a first approximation, to separately detect biological and non-biological

particles (Huffman et al., 2012; Pöhlker et al., 2012; Robinson et al., 2013). However, secondary organic aerosol (SOA), humic-like substance (HULIS), and other atmospheric materials have been suggested to interfere with detection of ambient biological particles via fluorescence (e.g. Huffman et al., 2010; Pöhlker et al., 2012; Gabey et al., 2013; Lee et al., 2013). In contrast, no real-time technique for PBAP analysis is able to comprehensively detect all classes of biological material. Microorganisms too large or too small for efficient collection by UV-LIF instrument will undercount these particles and some PBAP may fluoresce too weakly to be detected in many circumstances. Despite these physical uncertainties, measurements in the remote Amazon basin of Brazil showed that fluorescent particle number closely approximated biological particles measured by electron microscopy (Huffman et al., 2012), suggesting that techniques utilizing particle autofluorescence can be used in some geographic environments as first-approximation classifiers between biological and non-biological particles and can provide a lower limit for the atmospheric abundance of PBAP in the super-micron (> 1 μm) size range. More work is needed to better understand the scenarios in which this assumption holds.

This study represents the first co-located ambient deployment of the UV-APS and WIBS-4 instruments. Results suggest a good qualitative comparison between the two real-time techniques as well as with optical microscopy measurements performed on samples simultaneously collected via impaction. The comparisons reported here help characterize real-time fluorescence instrument capabilities for atmospheric bioaerosol measurement and will improve the ability of the atmospheric research community to reliably detect PBAP.

2. Methodology

2.1 Location of sampling site

Sampling was performed between 2 August and 2 September 2010 within Killarney National Park (KNP), Kerry, which is situated in south-west Ireland (N 52°01.263' W 09°30.553'). The site was located on the eastern perimeter of Reenadinna Woods, in a small clearing (~30 x 50 m) of manicured grass surrounded by *Taxus baccata*, Yew trees, and within meters of Muckross Lake (online supplemental material, Figure S1). KNP is one of the western-most European national parks. The site can be characterized as clean and rural, with local south-westerly winds and incoming air

masses influenced most heavily from pristine Atlantic trajectories, including minimal influence from anthropogenic emissions. The site comprises mixed deciduous trees and rich undergrowth. A list of typical botanic species found in Reenadinna Woods is outlined elsewhere (Kelly, 1981).

All instruments were housed in a purpose-built mobile laboratory trailer (3 m length) which was positioned immediately adjacent to a lawn area in front (~5 m) of the unoccupied Arthur Vincent House from where electrical power was obtained. Sample inlets extended vertically from the mobile laboratory were approximately 2.5 – 3.0 m in height above ground level and positioned approximately 4 m from the nearest trees.

2.2 Instrumentation

2.2.1 WIBS

The waveband integrated bioaerosol sensor Model 4 is a prototype of a series of real-time biological particle sensors developed by the University of Hertfordshire in the United Kingdom (Kaye et al., 2005; Foot et al., 2008; Gabey et al., 2011; Stanley et al., 2011; Healy et al., 2012a; 2012b). Briefly, the WIBS-4 consists of a central optical chamber, around which are arranged: (i) a continuous-wave 635 nm diode laser used for the initial detection of particles and the determination of particle size (optical diameter); (ii) a forward light-scattering quadrant photomultiplier used in the determination of particle size and asymmetry; and (iii) two pulsed xenon flashtube UV sources emitting sequentially at 280 nm and 370 nm. Fluorescence emission is detected in two bands: 310–400 nm (band 1) and 420–650 nm (band 2). Thus, for each particle, three fluorescence measurements are provided: (i) excitation at 280 nm, emission in band 1 (FL1); (ii) excitation at 280 nm, emission in band 2 (FL2); and (iii) excitation at 370 nm, emission in band 2 (FL3). For each individual particle detected, the instrument also provides the optical particle size (D_o) and the particle asymmetry factor (A_f), which is a parameter that describes the degree of symmetry for the forward scattered light (Kaye et al., 2005). Light detected by a four-quadrant photomultiplier tube (PMT) is combined to calculate an A_f; a spherical particle has A_f of 0, and rod-shaped fibres yields A_f near 100 (Gabey et al., 2010).

The particle counting efficiency of the WIBS-4 used in the current study drops below unity at $D_o < 0.69$ µm with D_{50} at 0.49 µm (Healy et al., 2012b). Therefore, number

concentrations for particles with $D_o < 0.69$ μm should be considered as lower limit values. The upper size limit is defined as a function of the PMT gain setting and was approx. 13 μm for this study. It is possible to operate the Hertfordshire WIBS-4 instruments at a different gain setting for the detection of particles up to approximately 31 μm in diameter. However, the configuration utilized here only permits optical particle sizing of particles between approx. 0.5 and 13 μm.

The trigger threshold setting of WIBS-4 (Trig) is an instrumental parameter that can be adjusted to predefine the lower particle size limit for which the firing of the xenon UV flash lamps (i.e. fluorescence excitation) will be triggered. The effects of such adjustments, i.e. minimum particle size as a function of Trig setting, had not previously been explored in an ambient setting. Furthermore WIBS instruments manufactured by the University of Hertfordshire are each unique prototypes and therefore the operational settings are not necessarily comparable between instruments. Three Trig settings were used for the WIBS-4 during the campaign (see also Sect. 3.2). A Trig setting of 8 (2-5 Aug.) corresponded to minimum detectable particle size of 0.52 μm (channel ≥ 1; see supplemental Table S1). A Trig setting of 20 (5-18 & 27-31 Aug.) corresponded to a minimum particle size of 0.65 μm (channel ≥ 4). Lastly, a Trig setting of 30 (23-27 Aug. and 31 Aug.-2 Sept.) corresponded to a minimum particle size of 0.75 μm (channel ≥ 6).

The performance of the two Xe flashtubes within the WIBS-4 was monitored throughout the measurement period. Flashtube power output values were recorded; upper and lower limit values were determined as ± 3σ (as standard deviation) from the mean. All particles resulting from UV flashes with power outside these bounds were eliminated from the fluorescent particle number concentration calculations. Note, however, that the total particle concentrations remained unaffected.

2.2.2 UV-APS

An ultraviolet aerodynamic particle sizer was utilized and operated using standard procedures (e.g. Huffman et al., 2010) and thereby provided 5-minute ensemble averages of number concentration, fluorescence intensity, and size of particles (Hairston et al., 1997; Brosseau et al., 2000). Aerodynamic particle sizing (D_a) in the diameter range between 0.5 and 20 μm is obtained by measuring time of particle

flight between two red (633 nm) He-Ne interrogating lasers. Optical excitation of the individual particles is provided by a pulsed Nd:YAG laser operating at 355 nm. Subsequent fluorescence is collected in a single bin (not wavelength dispersed) within the wavelength range between 420 and 575 nm. UV-APS particle transmission drops below unity at approximately 0.8 μm, with D_{50} approx. 0.54 μm (Huffman et al., 2012), and thus particles smaller than approximately 1 μm are conservatively treated as lower limit values.

2.2.3 Real-time fluorescence instrument comparison

Both WIBS-4 and UV-APS instruments sampled ambient air from the same inlet as shown in Figure S2. The vertical inlet line consisted of 0.5 inch stainless steel tube and was connected to a 0.5 inch Y-splitter with Swagelok fittings. Connections to both instruments after the split were made using conductive rubber tubing with an internal diameter of approx. 0.75 inch (Simolex Rubber Corp., Plymouth, MI). A by-pass flow of 2.4 L min^{-1} was drawn through a Swagelok tee (at 90^{o}) from the WIBS-4 line to match flows at 4.8 L min^{-1} on either branch of the Y-junction. Flow rates were regularly checked throughout the sample line with an external flowmeter (TSI Inc. Model 4140 Thermal Mass Flowmeter). The instruments and auxiliary pump pulled a total flow of 9.6 L min^{-1} through the inlet.

The WIBS-4 records the size of each individual particle sampled, but particles were binned according to UV-APS particle size channels for ease of comparison. Integrated particle number concentrations for each instrument are given for the size range greater than 1 μm in all cases here. A summary of the characteristic features and settings used by both WIBS-4 and UV-APS as operated here are outlined in Table 1.

The detection limit for each fluorescence channel of the WIBS-4 is defined as the mean fluorescence signal detected during > 10 min. of forced trigger data acquisition mode with no particle flow (i.e. pump off) (Gabey et al., 2010). Hence for each fluorescence channel (FL1, FL2, and FL3) the measured detection limit is taken as the minimum fluorescence intensity that can be reliably obtained by WIBS-4. In contrast the UV-APS bins the fluorescence intensity of individual particles into one of 64 channels. Particles with no measured fluorescence signal appear in channel 1. For the

current study particles that give fluorescence signals in channels >3 were defined as FBAP (Huffman et al., 2010).

WIBS-4 PMT voltage values were 0.701 V for FL1 and 0.649 V for both FL2 and FL3. The UV-APS PMT voltage was set 380 V as set by the factory to exclude polystyrene latex spheres (PSL) from being characterized as fluorescent. Increasing the UV-APS PMT setting allows for more sensitive detection of particle fluorescence, but also increased the likelihood of weakly fluorescent non-biological particles being counted as FBAP.

2.2.4 Sporewatch particle impactor

The Burkard Sporewatch Sampler (Burkard Scientific, UK) is a volumetric Hirst-type particle trap that operates by drawing air in through an orifice at a constant rate (10 L min^{-1}), allowing particles to impact onto silicone-coated tape (Lanzoi) mounted on a rotating drum (Hirst, 1952). The sampler was mounted on the roof of the mobile laboratory trailer (sampling height ~3 m above ground) and operated to rotate at a rate of one revolution per week, with start and end times manually recorded. Tapes were changed weekly, stored in air-sealed bags at ~4^{o}C and then cut into seven daily segments for analysis. Tape segments were mounted on microscope slides and counts of the identifiable fungal spores and pollen species were recorded. Microscope slides were stained with fuchsine (Sigma Aldrich) and the samples were examined under x400 magnification using an optical light microscope (VWR, TR500) according to regulations of the British Aerobiology Federation (Lacey and Venette, 1995). A longitudinal counting method was used, meaning that microscopic observation was performed in one continuous sweep through the centre of the 24 hour tape. Only 3% of the total tape area is observed at a given time by this method and particle concentrations are scaled accordingly. A more detailed description of the method is described elsewhere (Sterling et al., 1999; Lacey and West, 2007). Count values were converted into atmospheric number concentrations by scaling to the full tape width and dividing by the volumetric flow rate of the sampler after assuming that particles were deposited onto the tape with unit efficiency. Resultant concentrations are listed as counts per cubic centimeter of air (cm^{-3}).

Particle counting by this technique is done manually, and so several biases are possible. First, both the sensitivity and selectivity of the characterization is user-dependent. In this case, fungal spores and pollen grains were investigated and counted. Particles smaller than approximately 2 μm were not counted. Individual bacteria or small bacterial agglomerates, for example, would thus not have been counted by this method. Further, many fungal spores are hyaline (translucent, glassy appearance when examined by microscope) in nature and are therefore difficult to enumerate via optical microscopy. Lastly, the collection efficiency of the Sporewatch impactor drops below unity for particles smaller than approximately 3-5 μm (Khattab and Levetin, 2008). For these reasons, particle concentration values reported here should be taken as lower limit values.

2.2.5 MOUDI particle impactor

Size-resolved particle samples were collected using a micro-orifice uniform deposition impactor (MOUDI; MSP, model 110) at a flow-rate of 30 L min^{-1} via a dedicated inlet. Cut points of aerosol size fractionation have been discussed elsewhere (Marple et al., 1991). Samples were collected onto glass microscope slides for subsequent analysis via fluorescence microscopy.

2.2.6 Fluorescence microscopy

Fluorescence microscopy images were taken using a BZ-9000 Fluorescence Microscope (Keyence, Inc., Osaka, Japan). The instrument was equipped with a super high-compression mercury lamp (120 W) and a 2/3-inch, 1.5 mega pixel monochrome CCD. The following fluorescence filters were used to take images in different spectral ranges: OP-66834 DAPI-BP (λ_{ex} =360/20 nm, $\lambda_{Dichroic}$ =400 nm, λ_{Absorp} =460/25 nm), OP-66836 GFP-BP (λ_{ex} =470/20 nm, $\lambda_{Dichroic}$ =495 nm, λ_{Absorp} =535/25 nm), OP-66838 TexasRed (λ_{ex} =560/20 nm, $\lambda_{Dichroic}$ =595 nm, λ_{Absorp} =630/30 nm). Filter specifications are represented as wavelength and peak width (λ/FWHM).

2.2.7 Meteorological Data

Wind speed, wind direction, temperature, humidity, down-welling solar radiation, and rainfall were monitored using a Casella NOMAD weather station mounted on the roof of the mobile laboratory trailer. Measurements were made at 5 minute intervals.

3 Results and Discussion

3.1 Total particle comparison

The WIBS-4 and UV-APS instruments were operated continuously behind the same inlet for approximately one month. Mean coarse particle number concentration ($N_{T,c}$, $D > 1$ μm) was 32.8 and 32.4 cm^{-3} for WIBS-4 and UV-APS, respectively (Fig. 1), suggesting that there were no significant differences in sampling losses between the two branches of the inlet flow. Figure 1 also shows the correlation of total particle concentration between the instruments, averaged into 5-minute samples. The quantitative comparison between the instruments is good, with R^2 value of 0.90 over the campaign. The slope of 0.86, however, suggests that the WIBS method undercounted the total particle concentrations with respect to the UV-APS, especially at concentrations above approx. 50 cm^{-3}. The shallow slope to the correlation above 50 cm^{-3} is likely a result particle coincidence that reduced particle counts within the WIBS at a lower concentration than within the UV-APS as a result of differing physical instrument parameters. Size-resolved total particle concentrations measured throughout the campaign by both instruments are shown in Figure S3.

3.2 Overview of fluorescent aerosol trends

A comprehensive overview of biological particle measurements from Sporewatch/optical microscopy, WIBS-4, and UV-APS methods as employed over the whole measurement period is shown in Figure 2. A coarse view of the measurements shows broad agreement between the techniques, with rhythmic, synchronous increases in particle number across platform and wavelength channel in addition to episodic events of high concentration. Step-functions in the lower size of fluorescent particles from the FL1 channel (Fig. 2b) highlight periods when different trigger values were used to investigate optimal WIBS-4 operation (Sect. 2.2.1). Ignoring the corresponding fluctuation in lower particle size, as shown by the size-resolved image plots (Fig. 2) and by averaged size distributions from each channel (Fig. 3), the same pattern through time emerges.

The WIBS FL1 channel typically shows a broad, multi-modal distribution, with three distinct modes present for most of Aug. 5-18, and a bimodal distribution present for most of the rest of the campaign. The presence of the smallest mode (approx. 1.0 μm) during the period when the trigger value was set the lowest highlights the influence

that this WIBS setting has on the detection of particles and to the relative shape of fluorescent particle size distributions at small sizes. While discreet modes are present in the time-resolved size distributions (Fig. 2), these fine temporal differences are largely smoothed away when looking at average size distributions over the entire measurement period (Fig. 3a). The WIBS FL2 channel also shows a bimodal distribution, with consistent peaks at approx. 1 and 3 µm in particle size (Figs. 2c and 4b).

The size distributions from the WIBS FL3 channel and UV-APS, in contrast to WIBS FL1 and FL2 channels, show much stronger signal at the 3 µm particle size and relatively minimal influence from the 1 µm mode. The qualitative correlation in particle size between WIBS FL3 and UV-APS signals is expected, because the excitation wavelengths (370 nm and 355 nm, respectively) are both designed to highlight molecules related to active cellular metabolism (e.g. NAD(P)H and riboflavin) (Harrison and Chance, 1970; Setlow and Setlow, 1977; Eng et al., 1989; Li et al., 1991). There is no doubt that the assumption, that detecting fluorescence from these channels implies the presence of actively metabolizing cells, significantly over-simplifies the perspective of airborne microorganisms (Pöhlker et al., 2012; 2013). The broad nature of fluorescence excitation and emission spectra along with the relative similarity of excitation wavelength between these channels of the two instruments leads to broad consistency between the WIBS FL3 and UV-APS trends. However, despite the relative agreement between the peaks and temporal patterns of WIBS FL3 and UV-APS, Figure 3c and 3d show significantly reduced presence of the 1.2 µm mode in UV-APS compared to the WIBS FL3. This suggests that the UV-APS was less sensitive to smaller fluorescent particles, and thus may not record particles <2 µm as efficiently as the WIBS-4. The influence of particle size on fluorescent particle detection is likely a result of the fact that fluorescence detected from individual particles scales as a function of the 2^{nd} to 3^{rd} power of particle diameter, depending on the depth of excitation photon penetration into the interrogated particle (Tanke et al., 1982; Hill et al., 2001; Sivaprakasam et al., 2004). Further, the UV-APS is typically operated with relatively poor sensitivity in order to reduce the possible inclusion of non-biological artefacts in the fluorescence measurement (Huffman et al., 2012).

Both FL1 and FL2 channels are a result of excitation at 280 nm, which can probe proteins, amino acids, and other bio-fluorophores. The differences between FL1 (λ_{em} 310 – 400 nm) and FL2 (λ_{em} 420 – 650 nm) channels, however, can highlight different molecules. For example, Pöhlker et al. (2012) show that the FL1 band is much more efficient at detecting certain amino acids and proteins, whereas the FL2 channel detects flavin compounds (naturally occurring pigments, including riboflavin) at higher efficiency. This may also explain the qualitative overlap between the FL2 channel with aspects of each of the FL1 and FL3 channels, while the FL1 and FL3 channels show relatively little similarity in size distribution.

A quantitative comparison between the fluorescence channels detected is provided in Figure 4, each WIBS channel shown with respect to UV-APS fluorescent particle number. As discussed, of all WIBS channels, FL3 $N_{F,c}$ displays the highest correlation with UV-APS $N_{F,c}$ (R^2 0.78). The correlation between FL2 and UV-APS was also quite high (R^2 0.68), but between FL1 and UV-APS the correlation was poor (R^2 0.34). As mentioned, the good correlation between FL3 and UV-APS is expected, because of the common excitation and emission wavelengths employed by the two measurements. However, the UV-APS undercounts the FL3 measurement by a factor of 2.7 (Fig. 4d). In contrast the WIBS FL1 and FL2 signals result from fundamentally different fluorophores that result in much higher number concentrations.

Results of the Sporewatch analysis show qualitative agreement with temporal cycles from the single particle fluorescence measurements (Fig. 2, 5); when each of the real-time fluorescence channels peak, a corresponding peak in spore concentrations can be seen as well. Correlation analysis discussed later highlights the agreement further (Fig. 6). A comparison of the diurnal cycles will be discussed in Section 3.3. It is of note that the differing time resolution of the techniques used (5 min for real-time fluorescence instruments, 2 hr for Sporewatch) results in small temporal shifts in peaks of number concentrations.

3.3 Real-time fluorescence sensors versus Sporewatch

The advantage of the Sporewatch technique paired with optical microscopy is that number concentrations of individual microorganism types can be directly measured as a function of time. The most commonly observed species (2-10 μm) at the KNP site

during this experiment were all fungal spores: *Cladosporium spp.*, *Ganoderma spp.*, basidiospores., and ascospores. Ascospores are specific to fungi classified as ascomycetes which are ubiquitous in terrestrial ecosystems worldwide. Basidiospores are a reproductive spores produced by Basidiomycete fungi and *Ganoderma* is a genus of polypore mushrooms which grow on wood. Figure 2 shows a comparison of these species (with *Ganoderma* included in the Other category) alongside the size-resolved image plots of each fluorescence channel from the two real-time fluorescence instruments. The correlation of total biological particle concentration (Sporewatch) with WIBS and UV-APS may be more readily seen by comparing integrated number concentrations, however, as shown in Figure 5. $N_{F,c}$ determined by WIBS FL2, FL3 and UV-APS, respectively, each show similar periods of high and low concentrations (Fig. 5b), though each channel is plotted with a different y-scale multiplier. This suggests that, despite the differing lists of fluorophores accessible to each channel, the groups of microorganisms selected are similar. The differing magnitude to the numbers, however, suggests that individual particles in each group possessing lower fluorescence emission are likely to be under-counted by the measurements and that the sensitivity of the detection scheme is important. The rise and fall of the Sporewatch peaks at similar time periods of the FL2, FL3, and UV-APS $N_{F,c}$ suggests a good qualitative comparison between the techniques and that these channels of the real-time fluorescence instruments are indeed successful in detecting biological aerosols such as these fungal spores.

In contrast to the qualitative similarity of the temporal trends of the WIBS FL2, FL3, and UV-APS numbers with the spore concentrations, the WIBS FL1 numbers bear little temporal similarity (Fig. 5a). $N_{F,c}$ from FL1 is influenced heavily by particles with $D < 2$ µm, which is collected less efficiently by the Sporewatch impactor. Thus the population of particles detected by FL1 is largely separate from that of the particles observed by the paired Sporewatch/microscopy technique. These could be single or agglomerated bacteria particles that would be expected to fluoresce after excitation by 280 nm light of the FL1 channel. Though bacteria were not counted directly by the Sporewatch technique and their numbers cannot be accurately determined by the UV-APS or WIBS, the number of fluorescent particles 1 – 2 µm in the WIBS FL1 channel is approx. 10^5 m^{-3}, which is an order of magnitude higher than ~10^4 m^{-3} commonly estimated as the concentration of bacteria present over vegetated

surfaces (Bauer et al., 2002; Burrows et al., 2009b; Després et al., 2012). The cited studies estimated the concentration of bacteria over vegetated surfaces by reviewing a large number of studies collectively, each of which use different methods of detection, e.g. DNA sequencing, compared to the current work which uses online particle autofluoresence detection. Thus, it is likely that bacteria were detected by the WIBS FL1 channel, but that bacteria cannot explain all particles measured by theFL1 signal. We hypothesize three other mechanisms by which observed Sporewatch numbers would be lower than WIBS FL1 number. First, sea spray enriched in sub-micron organic material, including proteins and other biological degradation products (Prather et al., 2013), coating larger particles account for some of the FL1 particles and fluorescent coatings on particles observed via fluorescent microscopy. Second, low Sporewatch numbers are partially a result of hyaline particles not easily seen or counted using microscopy, but which could still fluoresce. This mechanism is less likely, however, because the process of fluorescent excitation is limited to particles that absorb, and so an individual particle would be expected to absorb strongly at 280 nm, but not so for visible (> 390 nm) identification. It is also unlikely that such biological particles would coincidentally fluoresce after 280 nm excitation, but not fluoresce with 355 – 370 nm excitation at the same time as being missed by visual counting. A third and final mechanism to explain the discrepancy between FL1 and Sporewatch number concentrations is that the FL1 channel counts a much higher number of non-biological particles that reduce the correlation with spore concentrations. These particles could be certain types of absorbing brown carbon secondary organic aerosol (Bones et al., 2010; Gabey et al., 2013; Lee et al., 2013) or soot particles (Lewitzka and Niessner, 1995; Panne et al., 2000), as adsorbed coatings (Huffman et al., 2012) or as discreet particles of size < 2 µm.

A quantitative view of the same correlations is shown in Figure 6; $N_{F,c}$ from each channel plotted against a subset of the Sporewatch number (all classes except *Cladosporium*). In this case, the correlation of $N_{F,c}$ from the UV-APS is the highest with the spore numbers (R^2 0.71), compared with R^2 of 0.05, 0.29, and 0.38 for WIBS FL1, FL2, and FL3 channels, respectively. In each comparison, however, the spore numbers are shown to undercount the real-time fluorescence measured numbers by factors of 3 to 14 (see Fig. 6 caption). This undercounting is likely influenced heavily by the fact that the Sporewatch does not efficiently collect particles with D < 2 µm, a

size range that contain significant particle numbers measured by several of the fluorescence channels (Fig. 3). The Sporewatch undercounting of small particles is unlikely to be the only cause of the scaling factor, however, because the UV-APS did not show significant fluorescent particles in this size range, but still under-counted spores by a factor of 3. As a result, it may indicate that other fluorescent bioparticles (e.g. bacteria) or non-biological particles in the same size range can be associated with the same air masses, and thus would increase $N_{F,c}$ but not the contemporaneous spore numbers.

3.4 Diurnal trends and atmospheric implications

To highlight the similarity of each of the measurements styles, Figure 7 shows diurnal (24 hr) plots of spores observed (Fig. 7a) and of each fluorescence channel (Figs. 7b-e). Each measurement shows an increase in biological or fluorescent number concentration during the night and early morning hours (approx. 02:00 – 06:00 LT), with daily minima occurring in the mid-afternoon (approx. 15:00 LT). Figure 7 also shows the corresponding diurnal trend in relative humidity, which peaks at similar hours. This is consistent with commonly observed trends that many bioparticle classes correlate strongly with RH and peak at night due to active fungal emission mechanisms that require high humidity to function (e.g. Hirst, 1953; Rockett and Kramer, 1974; Huffman et al., 2012; Schumacher et al., 2013; Toprak and Schnaiter, 2013). The UV-APS and WIBS FL3 channels each show mono-modal size distributions peaking at 3-4 µm through the night, while the FL2 channel shows a bio-modal distribution peaking at approx. 1 µm and 3-4 µm in size. These diurnal trends are reflected strongly by the concentrations of basidiospores and even more so by ascospores. Based on the observations via optical microscopy, the larger species (D ~3-4 µm) identified by the real-time fluorescence techniques are likely to be basidiospores and *Ganoderma spp.*, while the smaller mode (D approx. 1 µm) observed for the FL2 channel may be comprised of ascospores. However, the identity of the smaller fluorescent particles is more uncertain, because the particles are relatively unidentifiably via optical microscopy because of insufficient magnification. Huffman et al. (2012) argue, using diurnal measurements and comparison with previous literature reports, that $N_{F,c}$ from UV-APS observations in the Amazon rainforest are most likely to be a mixture of ascospores and basidiospores. Though measurements were conducted in a very different ecosystem, the conclusions here are

consistent with earlier suggestions that UV-LIF measurements are particularly well suited to the detection of these bioparticle classes. Further, Manninen et al. (2014) present multi-year Sporewatch measurements in Hyytiälä, Finland and show that late summer (August and September) in N. Europe are peak seasons for many spores, including several groups of ascospores and basidiospores. Comparing with long-term UV-APS measurements reported by Schumacher et al. (2013) and Manninen et al. (2014) suggest these classes of spores peak on a similar yearly cycle as the UV-APS $N_{F,c}$, and thus the August measurement period in this study coincides with a period of the year consistent with high fungal spore concentrations. Further, the fungal spore concentrations reported by Manninen et al. of $1 – 10 \times 10^4$ m^{-3} ($1\text{-}10 \times 10^{-2}$ cm^{-3}) are within an order of magnitude of Sporewatch numbers reported here $0.1\text{-}1 \times 10^{-2}$ cm^{-3}.

Diurnal patterns for additional meteorological measurements (e.g. air temperature, solar radiation, atmospheric pressure, and wind speed) observed during the entire measurement period are shown in supplemental Figure S4. A consistent diurnal cycle was observed for RH with night time periods (campaign max. 98%) reaching higher values than during the day (campaign min. 38 %). Minimum and maximum air temperatures recorded during the campaign were 4 °C and 26 °C, respectively, with a campaign average of 15 °C. Generally calm weather conditions, with several short periods of rain, were encountered throughout the entire campaign. This general pattern was reflected meteorologically by the lack of observable diurnal patterns for atmospheric pressure and also by low wind speeds.

3.5 Weakly detected Cladosporium spores

In contrast to the diurnal trend of the ascospores and basidiospores, the "Other" category shows relatively flat diurnal profile, and the concentration of *Cladosporium spp.* spores, which are among the most common spore types in vegetated areas, shows a relative increase during the middle of the afternoon (peaking approx. 14:00). This temporal pattern for *Cladosporium* is expected and has been reported frequently. It is usually considered to be a dry weather spore whose concentration increases during warm periods of low relative humidity (De Groot, 1968; Oliveira et al., 2009). The interesting observation here is that the real-time fluorescence methods are relatively insensitive to the increases in *Cladosporium* spore concentration. Correlation plots of each fluorescence channel with *Cladosporium* spores show no qualitative pattern,

562 with R^2 values < 0.006 in all cases. The reason for the relative insensitivity of these
563 techniques to *Cladosporium* is unknown, but may relate to the dark-skinned (i.e.
564 absorbing) nature of these spores preventing impinging photons from penetrating
565 exterior pigments to excite fluorescence from internal fluorophores (Bell-Pedersen et
566 al., 1996).
567
568
569 *3.6 Marine particle influence*
570 Fluorescence microscopy images of size-resolved MOUDI stages collected during the
571 study qualitatively show the presence of spores and other biological particles. The
572 particles in the size range > 2 μm observed by the fluorescent microscopy technique
573 to have the highest fluorescence were identified morphologically as PBAP. Many of
574 the strongly fluorescent PBAP also demonstrated a clear cell wall fluorescence which
575 suggests that it is not the cytosol or cellular metabolites such as NAD(P)H or
576 riboflavin, but structural components of the cell wall that dominate the emission
577 (Pöhlker et al., 2012; 2013). Many of the fluorescent PBAP also demonstrated fungal
578 spore- like morphologies. Also frequently observed, however, were cubic particles
579 that appear morphologically similar to NaCl (Fig. 8), and needle-like particles
580 consistent with structures of crystals such as $CaSO_4$. No elemental analysis was
581 possible on these particle agglomerates for confirmation, however. The observations
582 of these inorganic-appearing particles suggest the influence of marine air containing
583 sea salt. Of further interest is the appearance of bioparticles attached to the cubic salt-
584 like particles, in which cases the bioparticle typically fluoresces strongly while the sea
585 salt-like crystals do not. The number concentration of bioparticles and sea salt in the
586 coarse particle mode make the agglomeration of these particles while airborne
587 statistically unlikely. Thus, we suggest that the bioparticle-salt agglomerates were
588 likely emitted by marine sources and transported approx. 20 km from the ocean west
589 of Ireland (Kenny and Jennings, 1998; Aller et al., 2005).
590
591 **4 Conclusions**
592 The study shows the measurement capabilities of the WIBS-4 and UV-APS to detect
593 biological particles in a rural, ambient location and is the first to compare these two
594 commercial sensors. Information revealed by each instrument is qualitatively similar,
595 but key differences are apparent. Total coarse particle concentration ($N_{T,c}$) was shown

to correlate well between the two instruments, and size distributions of total particles were similar. The UV-APS sizing measurement (aerodynamic diameter) showed more highly resolved distributions than did the WIBS-4 (optical diameter). This is likely a function of the physical properties of the particle sizing schemes in each instrument, and has been suggested previously. The minimum particle size detected by the WIBS-4, however, is related to the trigger threshold selected by the operator.

Concentrations of fluorescent particles observed during the measurement period by both instruments show regular, diurnal fluctuations that are qualitatively similar to each other. Differences in excitation/emission wavelength result in different particle populations observed, however. The UV-APS (λ_{ex} 355 nm) and WIBS FL3 channel (λ_{ex} 370 nm) correlate strongly, suggesting that the relative proximity of the excitation wavelengths allows each of these channels to excite similar fluorophores within interrogated particles. The UV-APS and WIBS FL3 channel show fluorescent particles dominated by a mode peaking at approx. 3 µm, with additional presence of a mode at approx. 1 µm present in FL3. The UV-APS $N_{F,c}$ was lower than FL3 $N_{F,c}$ by a factor of approx. 2.4, however, suggesting that the UV-APS particle detection sensitivity was relatively poor.

The WIBS FL2 channel showed a consistently bi-modal distribution comprised of 1 and 3 µm modes and qualitatively appears to be a combination of modes present in the FL1 and FL3 channels. The WIBS FL2, FL3, and UV-APS particle numbers correlated well in time and number with spore numbers collected via Sporewatch impactor and enumerated via optical microscopy. Each showed a diurnal peak in the early morning, with daily minima in the mid afternoon.

The WIBS FL1 channel, however, showed very different patterns. FL1 showed a relatively consistent diurnal pattern and a multi-modal size distribution with the highest concentration of fluorescent particles observed by any channel, but with the poorest correlation with spore numbers. This arises partially, because $N_{F,c}$ from FL1 was summed of particles with D > 1 µm, whereas the Sporewatch impaction technique is relatively inefficient at collecting particles < 2 µm. The smaller particles that escape Sporewatch detection, but that are recorded by the FL1 channel (λ_{ex} 270 nm) may include bacterial cells and protein-enriched coatings from sea spray origin.

However, the discrepancy could also indicate the detection of non-biological particles such as certain absorbing SOA or soot into the FL1 particle number. It is thus clear from these observations that the multiple channels of fluorescent information delivered by the WIBS provide an advantage over the single fluorescence channel of the UV-APS. The qualitative similarity of diurnal patterns and of the UV-APS with WIBS FL3 channels highlights the utility of the UV-APS to detect the overall trends of fluorescent biological particles, however.

Comparisons between the real-time fluorescence instruments and the Sporewatch/microscopy technique reveal that the most likely species of airborne microorganism (D > 2 µm) present in Killarney National Park during the measurement period were spores, including basidiospores, ascospores, *Ganoderma spp.*, and *Cladosporium spp*. The correlation of total spore concentration with the WIBS FL2, FL3, and UV-APS $N_{F,c}$ was high. However, *Cladosporium* spores correlated extremely poorly with all fluorescent measurements, suggesting that dark-walled cell walls may inhibit real-time fluorescence detection. Despite the presence of the spores observed, the microscopy results cannot rule out the possible contribution of soil bacteria such as actinobacteria and streptomycetes in the size range 1 – 2 µm that is not efficiently collected by the Sporewatch. These commonly airborne PBAP classes could also contribute to $N_{F,c}$ and reduce correlation with Sporewatch number.

The results of this study show that both WIBS and UV-APS techniques are capable of providing real-time information about biological aerosol particles, and that they can relate the major temporal trends of airborne fungal spores. Significant uncertainties still remain in the interpretation of the data from these instruments, and follow-up studies (e.g. systematic comparisons of the instruments in a controlled laboratory setting) will be necessary to inform further studies and analysis. For example, further work will be required to understand the nature of the poor correlation between spore concentration and WIBS FL1 number. Additional follow-up work will also be necessary to understand WIBS triggering thresholds to best characterize both fluorescent and non-fluorescent aerosol in field environments with unknown aerosol. These data show that the instruments performed well in a relatively clean, rural national park in western Ireland, but operational considerations will likely be different

664 at sites more heavily influenced by anthropogenic aerosol sources. On the other hand
665 UV-APS detected few of the smaller bacterial PBAP because of its single excitation
666 wavelength. Measurements such as those presented here may provide direct inputs for
667 the improvement of global models investigating the role of PBAP as ice or cloud
668 condensation nuclei.
669
670 Relatively few estimates of PBAP concentrations exist, and the present study provides
671 measured concentrations in a rural European environment. Further, the comparison of
672 real-time fluorescence techniques capable of detecting fluorescent biological particles
673 at high time and size resolution are supported by good correlations with direct
674 observations of particles using optical microscopy (bright-field and fluorescence).
675 These data support the idea that real-time fluorescence techniques can significantly
676 improve time resolution and analysis time of traditional PBAP identification, which
677 can be very laborious, time-consuming, and costly. Spore concentrations were
678 observed on the order of $1 – 10 \times 10^4$ m^{-3}, which is consistent with previous estimates
679 (e.g. Elbert et al., 2007; Després et al., 2012; Manninen et al., 2014). Bacteria
680 concentrations were not directly measured by these techniques, but the number of 1 –
681 2 µm particles in the WIBS FL1 channel is on the order of 10^5 m^{-3}, which could easily
682 encompass the ~10^4 m^{-3} of bacteria commonly estimated to be present as a continental
683 background concentration (Bauer et al., 2002; Burrows et al., 2009b; Després et al.,
684 2012). Observations that spore and FBAP concentrations cycle on a daily basis with
685 RH and inversely with temperature are consistent with many previous reports that
686 suggest many classes of fungal spores utilize periods of high humidity for active
687 release (Jones and Harrison, 2004; Pringle et al., 2005; Elbert et al., 2007). Lastly,
688 fluorescent microscopy images of sea salt-like particles agglomerated with biological
689 cells suggests that air at the site was influenced but marine air and that the ocean
690 provides one source for airborne biological material.
691

692 **5. Acknowledgements**

693 The authors acknowledge the National Parks and Wildlife Service of Ireland for
694 providing a sampling location in Killarney National Park with a suitable power
695 supply. This work was financially supported by the Irish EPA BioCheA 2007 CCRP
696 Project 4.4.6 and STRIVE Doctoral training program (2008-PhD-AQ-2). Financial
697 support for J. A. Huffman, C. Pöhlker, and U. Pöschl was from the Max Planck

698 Society, the Max Planck Graduate Center with the Johannes Gutenberg-Universität
699 Mainz (MPGC), and the LEC Geocycles Mainz. J. A. Huffman acknowledges internal
700 faculty funding from the University of Denver. The authors also acknowledge: J.
701 Schneider and S. Borrmann (MPIC Particle Chemistry) for providing a UV-APS
702 instrument; Eoin McGillicuddy, Ian O'Connor and Arnaud Allanic for help with the
703 mobile laboratory and help transporting equipment. P. Kaye, W. Stanley are
704 acknowledged for their technical support provided to project BioChea while David
705 Dodd is acknowledged for his support of project BioChea.

6. References

Aller, J. Y., Kuznetsova, M. R., Jahns, C. J. and Kemp, P. F.: The sea surface microlayer as a source of viral and bacterial enrichment in marine aerosols, Journal of Aerosol Science, 36, 801-812, http://dx.doi.org/10.1016/j.jaerosci.2004.10.012, 2005.

Bauer, H., Kasper-Giebl, A., Löflund, M., Giebl, H., Hitzenberger, R., Zibuschka, F. and Puxbaum, H.: The contribution of bacteria and fungal spores to the organic carbon content of cloud water, precipitation and aerosols, Atmospheric Research, 64, 109-119, 2002.

Bell-Pedersen, D., Garceau, N. and Loros, J. J.: Circadian rhythms in fungi, Journal of Genetics, 75, 387-401, 1996.

Bones, D. L., Henricksen, D. K., Mang, S. A., Gonsior, M., Bateman, A. P., Nguyen, T. B., Cooper, W. J. and Nizkorodov, S. A.: Appearance of strong absorbers and fluorophores in limonene-O-3 secondary organic aerosol due to NH4+-mediated chemical aging over long time scales, J. Geophys. Res.-Atmos., 115, 10.1029/2009jd012864, 2010.

Brosseau, L. M., Vesley, D., Rice, N., Goodell, K., Nellis, M. and Hairston, P.: Differences in detected fluorescence among several bacterial species measured with a direct-reading particle sizer and fluorescence detector, Aerosol Sci. Technol., 32, 545-558, 2000.

Burrows, S. M., Butler, T., Jockel, P., Tost, H., Kerkweg, A., Pöschl, U. and Lawrence, M. G.: Bacteria in the global atmosphere - Part 2: Modeling of emissions and transport between different ecosystems, Atmospheric Chemistry and Physics, 9, 9281-9297, 2009a.

Burrows, S. M., Elbert, W., Lawrence, M. G. and Pöschl, U.: Bacteria in the global atmosphere - Part 1: Review and synthesis of literature data for different ecosystems, Atmospheric Chemistry and Physics, 9, 9263-9280, 2009b.

Caruana, D. J.: Detection and analysis of airborne particles of biological origin: present and future, Analyst, 136, 4641-4652, 10.1039/c1an15506g, 2011.

Christner, B. C., Morris, C. E., Foreman, C. M., Cai, R. M. and Sands, D. C.: Ubiquity of biological ice nucleators in snowfall, Science, 319, 1214-1214, 10.1126/science.1149757, 2008.

De Groot, R. C.: Diurnal cycles of airborne spores produced by forest fungi, Phytopathology, 58, 1223-1229, 1968.

DeLeon-Rodriguez, N., Lathem, T. L., Rodriguez-R, L. M., Barazesh, J. M., Anderson, B. E., Beyersdorf, A. J., Ziemba, L. D., Bergin, M., Nenes, A. and Konstantinidis, K. T.: Microbiome of the upper troposphere: Species composition and prevalence, effects of tropical storms, and atmospheric implications, Proceedings of the National Academy of Sciences of the United States of America, 110, 2575-2580, 10.1073/pnas.1212089110, 2013.

745 Després, V. R., Huffman, J. A., Burrows, S. M., Hoose, C., Safatov, A. S., Buryak, G.
746 A., Fröhlich-Nowoisky, J., Elbert, W., Andreae, M. O., Pöschl, U. and Jaenicke, R.:
747 Primary Biological Aerosol Particles in the Atmosphere: A Review, Tellus Series B-
748 Chemical and Physical Meteorology, 64, 15598, 10.3402/tellusb.v64i0.15598, 2012.

749 Diehl, K., Quick, C., Matthias-Maser, S., Mitra, S. K. and Jaenicke, R.: The ice
750 nucleating ability of pollen - Part I: Laboratory studies in deposition and condensation
751 freezing modes, Atmospheric Research, 58, 75-87, 2001.

752 Elbert, W., Taylor, P. E., Andreae, M. O. and Pöschl, U.: Contribution of fungi to
753 primary biogenic aerosols in the atmosphere: wet and dry discharged spores,
754 carbohydrates, and inorganic ions, Atmospheric Chemistry and Physics, 7, 4569-
755 4588, 2007.

756 Eng, J., Lynch, R. M. and Balaban, R. S.: Nicotinamide Adenine Dinucleotide
757 Fluorescence Spectroscopy and Imaging of Isolated Cardiac Myocytes, Biophysical
758 Journal, 55, 621-630, 1989.

759 Eversole, J. D., Hardgrove, J. J., Cary, W. K., Choulas, D. P. and Seaver, M.:
760 Continuous, rapid biological aerosol detection with the use of UV fluorescence:
761 Outdoor test results, Field Anal. Chem. Technol., 3, 249-259, 1999.

762 Foot, V. E., Kaye, P. H., Stanley, W. R., Barrington, S. J., Gallagher, M. and Gabey,
763 A.: Low-cost real-time multi-parameter bio-aerosol sensors, Proceedings of the SPIE -
764 The International Society for Optical Engineering, 7116, 711601, 10.1117/12.800226,
765 2008.

766 Fröhlich-Nowoisky, J., Pickersgill, D. A., Despés, R. V. and Pöschl, U.: High
767 diversity of fungi in air particulate matter, Proceedings of the National Academy of
768 Sciences, 106, 12814 - 12819, doi: 10.1073/pnas.0811003106, 2009.

769 Fröhlich-Nowoisky, J., Burrows, S. M., Xie, Z., Engling, G., Solomon, P. A., Fraser, M. P.,
770 Mayol-Bracero, O. L., Artaxo, P., Begerow, D., Conrad, R., Andreae, M. O., Després, V. R.
771 and Pöschl, U.: Biogeography in the air: fungal diversity over land and oceans,
772 Biogeosciences, 9, 1125 - 1136, doi:10.5194/bg-9-1125-2012, 2012.

773 Gabey, A., Stanley, W. R., Gallagher, M. and Kaye, P. H.: The fluorescence
774 properties of aerosol larger than 0.8 μm in urban and tropical rainforest locations,
775 Atmospheric Chemistry and Physics, 11, 5491-5504, 10.5194/acp-11-5491-2011,
776 2011.

777 Gabey, A. M., Gallagher, M. W., Whitehead, J., Dorsey, J. R., Kaye, P. H. and
778 Stanley, W. R.: Measurements and comparison of primary biological aerosol above
779 and below a tropical forest canopy using a dual channel fluorescence spectrometer,
780 Atmospheric Chemistry and Physics, 10, 4453-4466, 10.5194/acp-10-4453-2010,
781 2010.

782 Gabey, A. M., Vaitilingom, M., Freney, E., Boulon, J., Sellegri, K., Gallagher, M. W.,
783 Crawford, I. P., Robinson, N. H., Stanley, W. R. and Kaye, P. H.: Observations of
784 fluorescent and biological aerosol at a high-altitude site in central France,

785 Atmospheric Chemistry and Physics, 13, 7415-7428, 10.5194/acp-13-7415-2013,
786 2013.

787 Haga, D. I., Iannone, R., Wheeler, M. J., Mason, R., Polishchuk, E. A., Fetch, T., Jr.,
788 van der Kamp, B. J., McKendry, I. G. and Bertram, A. K.: Ice nucleation properties of
789 rust and bunt fungal spores and their transport to high altitudes, where they can cause
790 heterogeneous freezing, J. Geophys. Res.-Atmos., 118, 7260-7272,
791 10.1002/jgrd.50556, 2013.

792 Hairston, P. P., Ho, J. and Quant, F. R.: Design of an instrument for real-time
793 detection of bioaerosols using simultaneous measurement of particle aerodynamic
794 size and intrinsic fluorescence, Journal of Aerosol Science, 28, 471-482, 1997.

795 Harrison, D. E. and Chance, B.: Fluorimetric Technique for Monitoring Changes in
796 Level of Reduced Nicotinamide Nucleotides in Continuous Cultures of
797 Microorganisms, Applied Microbiology, 19, 446-450, 1970.

798 Heald, C. L. and Spracklen, D. V.: Atmospheric budget of primary biological aerosol
799 particles from fungal spores, Geophysical Research Letters, 36, L09806,
800 10.1029/2009gl037493, 2009.

801 Healy, D. A., O'Connor, D. J., Burke, A. M. and Sodeau, J. R.: A laboratory
802 assessment of the Waveband Integrated Bioaerosol Sensor (WIBS-4) using individual
803 samples of pollen and fungal spore material, Atmospheric Environment, 60, 534-543,
804 10.1016/j.atmosenv.2012.06.052, 2012a.

805 Healy, D. A., O'Connor, D. J. and Sodeau, J. R.: Measurement of the particle
806 counting efficiency of the "Waveband Integrated Bioaerosol Sensor" model number 4
807 (WIBS-4), Journal of Aerosol Science, 47, 94-99, 10.1016/j.jaerosci.2012.01.003,
808 2012b.

809 Hill, S. C., Pinnick, R. G., Niles, S., Fell, N. F., Pan, Y. L., Bottiger, J., Bronk, B. V.,
810 Holler, S. and Chang, R. K.: Fluorescence from airborne microparticles: dependence
811 on size, concentration of fluorophores, and illumination intensity, Applied Optics, 40,
812 3005-3013, 2001.

813 Hirst, J. M.: An Automatic Volumetric Spore Trap, Annals of Applied Biology, 39,
814 257-265, 10.1111/j.1744-7348.1952.tb00904.x, 1952.

815 Hirst, J. M.: Changes in atmospheric spore content: Diurnal periodicity and the effects
816 of weather, Transactions of the British Mycological Society, 36, 375-393, IN378, Doi:
817 10.1016/s0007-1536(53)80034-3, 1953.

818 Ho, J.: Future of biological aerosol detection, Anal. Chim. Acta, 457, 125-148, 2002.

819 Hoose, C., Kristjansson, J. E. and Burrows, S. M.: How important is biological ice
820 nucleation in clouds on a global scale?, Environ. Res. Lett., 5, 024009, 10.1088/1748-
821 9326/5/2/024009, 2010.

822 Huffman, J. A., Treutlein, B. and Pöschl, U.: Fluorescent biological aerosol particle
823 concentrations and size distributions measured with an Ultraviolet Aerodynamic

824 Particle Sizer (UV-APS) in Central Europe, Atmospheric Chemistry and Physics, 10,
825 3215-3233, 2010.

826 Huffman, J. A., Sinha, B., Garland, R. M., Snee-Pollmann, A., Gunthe, S. S., Artaxo,
827 P., Martin, S. T., Andreae, M. O. and Poeschl, U.: Size distributions and temporal
828 variations of biological aerosol particles in the Amazon rainforest characterized by
829 microscopy and real-time UV-APS fluorescence techniques during AMAZE-08,
830 Atmospheric Chemistry and Physics, 12, 11997-12019, 10.5194/acp-12-11997-2012,
831 2012.

832 Huffman, J. A., Prenni, A. J., DeMott, P. J., Pöhlker, C., Mason, R. H., Robinson, N.
833 H., Fröhlich-Nowoisky, J. F., Tobo, Y., Després, V., Garcia, E., Gochis, D. J., Harris,
834 E., Müller-Germann, I., Ruzene, C., Schmer, B., Sinha, B., Day, D. A., Andreae, M.
835 O., Jimenez, J. L., Gallagher, M., Kreidenweis, S. M., Bertram, A. K. and Pöschl, U.:
836 High concentrations of biological aerosol particles and ice nuclei during and after
837 rain, Atmospheric Chemistry and Physics, 13, 6151-6164, 10.5194/acp-13-6151-
838 2013, 2013.

839 Hummel, M., Hoose, C., Gallagher, M., Healy, D. A., Huffman, J. A., O'Connor, D.,
840 Pöschl, U., Pöhlker, C., Robinson, N. H., Schnaiter, M., Sodeau, J. R., Toprak, E. and
841 Vogel, H.: Regional-scale simulations of fungal spore aerosols using an emission
842 parameterization adapted to local measurements of fluorescent biological aerosol
843 particles, Atmos. Chem. Phys. Discuss., 14, 9903-9950, 10.5194/acpd-14-9903-2014,
844 2014.

845 Jones, A. M. and Harrison, R. M.: The effects of meteorological factors on
846 atmospheric bioaerosol concentrations - a review, Science of the Total Environment,
847 326, 151-180, 10.1016/j.scitotenv.2003.11.021, 2004.

848 Kaye, P. H., Stanley, W. R., Hirst, E., Foot, E. V., Baxter, K. L. and Barrington, S. J.:
849 Single particle multichannel bio-aerosol fluorescence sensor, Optics Express, 13,
850 3583-3593, 2005.

851 Kenny, C. M. and Jennings, S. G.: Background bioaerosol measurements at Mace
852 Head, Journal of Aerosol Science, 29, S779-S780, 10.1016/S0021-8502(98)90572-9,
853 1998.

854 Khattab, A. and Levetin, E.: Preliminary studies on the effect of the Burkard alternate
855 orifice on airborne fungal spore concentrations. Aerobiologia, 2008. 24: p. 165-171.
856 Preliminary studies on the effect of the Burkard alternate orifice on airborne fungal
857 spore concentrations., Aerobiologia, 24, 165-171, 2008.

858 Lacey, J. and Dutkiewicz, J.: Bioaerosols and Occupational Lung Disease, Journal of
859 Aerosol Science, 25, 1371-1404, 1994.

860 Lacey, J. and Venette, J.: Outdoor Air Sampling Techniques, in: Bioaerosols
861 Handbook, edited by: Cox, C. S. and Wathes, C. M., Lewis Publishers, Boca Raton,
862 FL, 407 - 471, 1995.

863 Lacey, M. E. and West, J. S.: The air spora: a manual for catching and identifying
864 airborne biological particles, Springer, 2007.

865 Lee, H. J., Laskin, A., Laskin, J. and Nizkorodov, S. A.: Excitation–Emission Spectra
866 and Fluorescence Quantum Yields for Fresh and Aged Biogenic Secondary Organic
867 Aerosols, Environ. Sci. Technol., 47, 5763-5770, 10.1021/es400644c, 2013.

868 Lewitzka, F. and Niessner, R.: Application of Time-Resolved Fluorescence
869 Spectroscopy on the Analysis of PAH-Coated Aerosols, Aerosol Sci. Technol., 23,
870 454-464, 10.1080/02786829508965328, 1995.

871 Li, J. K., Asali, E. C. and Humphrey, A. E.: Monitoring Cell Concentration and
872 Activity by Multiple Excitation Flourometry, Biotechnology Progress, 7, 21-27, 1991.

873 Madelin, T. M.: Fungal Aerosols - A Review, Journal of Aerosol Science, 25, 1405-
874 1412, 10.1016/0021-8502(94)90216-x, 1994.

875 Maki, L. R., Glyan, E. L., Chang-Chien, M. M. and Caldwell, D. R.: Ice nucleation
876 induced by Pseudomonas syringae, Applied and Environmental Microbiology, 28,
877 456-459, 1974.

878 Manninen, H. E., Sihto-Nissilä, S.-L., Huffman, J. A., Bäck, J., Pessi, A.-M.,
879 Hiltunen, V., Aalto, P., Hidalgo, P. J., Hari, P., Saarto, A., Kulmala, M. and Petäjä,
880 T.: Annual pattern of airborne pollen grains, fungal spores and particle mass in a
881 boreal forest, Boreal Environmental Research, In Review, 2014.

882 Marple, V. A., Rubow, K. L. and Behm, S. M.: A microorifice uniform deposit
883 impactor (MOUDI) - description, calibration, and use, Aerosol Sci. Technol., 14, 434-
884 446, 10.1080/02786829108959504, 1991.

885 Möhler, O., DeMott, P. J., Vali, G. and Levin, Z.: Microbiology and atmospheric
886 processes: the role of biological particles in cloud physics, Biogeosciences, 4, 1059-
887 1071, 2007.

888 Morris, C. E., Georgakopoulos, D. G. and Sands, D. C.: Ice nucleation active bacteria
889 and their potential role in precipitation, Journal de Physique IV, 121, 87-103,
890 10.1051/jp4:2004121004, 2004.

891 Morris, C. E., Sands, D. C., Vinatzer, B. A., Glaux, C., Guilbaud, C., Buffiere, A.,
892 Yan, S., Dominguez, H. and Thompson, B. M.: The life history of the plant pathogen
893 Pseudomonas syringae is linked to the water cycle, ISME J, 2, 321-334, 2008.

894 Morris, C. E., Sands, D. C., Glaux, C., Samsatly, J., Asaad, S., Moukahel, A. R.,
895 Gonçalves, F. L. T. and Bigg, E. K.: Urediospores of rust fungi are ice nucleation
896 active at > -10 ^{o}C and harbor ice nucleation active bacteria, Atmospheric Chemistry
897 and Physics, 13, 4223-4233, 10.5194/acp-13-4223-2013, 2013.

898 Morris, C. E., Conen, F., Huffman, J. A., Phillips, V., Pöschl, U. and Sands, D. C.:
899 Bioprecipitation: a feedback cycle linking Earth history, ecosystem dynamics and
900 land use through biological ice nucleators in the atmosphere, Global Change Biology,
901 20, 341-351, 10.1111/gcb.12447, 2014.

902 Oliveira, M., Ribeiro, H., Delgado, J. and Abreu, I.: The effects of meteorological
903 factors on airborne fungal spore concentration in two areas differing in urbanisation

level, International Journal of Biometeorology, 53, 61-73, 10.1007/s00484-008-0191-2, 2009.

Pan, Y.-L., Hill, S. C., Pinnick, R. G., House, J. M., Flagan, R. C. and Chang, R. K.: Dual-excitation-wavelength fluorescence spectra and elastic scattering for differentiation of single airborne pollen and fungal particles, Atmospheric Environment, 45, 1555-1563, 10.1016/j.atmosenv.2010.12.042, 2011.

Pan, Y. L., Pinnick, R. G., Hill, S. C., Rosen, J. M. and Chang, R. K.: Single-particle laser-induced-fluorescence spectra of biological and other organic-carbon aerosols in the atmosphere: Measurements at New Haven, Connecticut, and Las Cruces, New Mexico, J. Geophys. Res.-Atmos., 112, 15, 10.1029/2007jd008741, 2007.

Panne, U., Knöller, A., Kotzick, R. and Niessner, R.: On-line and in-situ detection of polycyclic aromatic hydrocarbons (PAH) on aerosols via thermodesorption and laser-induced fluorescence spectroscopy, Fresenius J Anal Chem, 366, 408-414, 10.1007/s002160050083, 2000.

Patel, N. J. and Bush, R. K.: Role of environmental allergens in rhinitis, Immunology and Allergy Clinics of North America, 20, 323-353, http://dx.doi.org/10.1016/S0889-8561(05)70151-X, 2000.

Pinnick, R. G., Hill, S. C., Nachman, P., Pendleton, J. D., Fernandez, G. L., Mayo, M. W. and Bruno, J. G.: Fluorescence Particle Counter for Detecting Airborne Bacteria and Other Biological Particles, Aerosol Sci. Technol., 23, 653-664, 1995.

Pinnick, R. G., Hill, S. C., Pan, Y. L. and Chang, R. K.: Fluorescence spectra of atmospheric aerosol at Adelphi, Maryland, USA: measurement and classification of single particles containing organic carbon, Atmospheric Environment, 38, 1657-1672, 10.1016/j.atmosenv.2003.11.017, 2004.

Pöhlker, C., Huffman, J. A. and Pöschl, U.: Autofluorescence of atmospheric bioaerosols - fluorescent biomolecules and potential interferences, Atmospheric Measurement Techniques, 5, 37-71, 10.5194/amt-5-37-2012, 2012.

Pöhlker, C., Huffman, J. A., Förster, J.-D. and Pöschl, U.: Autofluorescence of atmospheric bioaerosols: spectral fingerprints and taxonomic trends of pollen, Atmospheric Measurement Techniques, 13, 3369-3392, 10.5194/amt-6-3369-2013, 2013.

Pöschl, U.: Atmospheric aerosols: Composition, transformation, climate and health effects, Angewandte Chemie-International Edition, 44, 7520-7540, 10.1002/anie.200501122, 2005.

Pöschl, U., Martin, S. T., Sinha, B., Chen, Q., Gunthe, S. S., Huffman, J. A., Borrmann, S., Farmer, D. K., Garland, R. M., Helas, G., Jimeney, J. L., King, S. M., Manzi, A., Mikhailov, E., Pauliquevis, T., Petters, M. D., Prenni, A. J., Roldin, P., Rose, D., Schneider, J., Su, H., Zorn, S. R., Artaxo, P. and Andreae, M. O.: Rainforest Aerosols as Biogenic Nuclei of Clouds and Precipitation in the Amazon, Science, 329, 1513-1516, 10.1126/science.1191056, 2010.

Prather, K. A., Bertram, T. H., Grassian, V. H., Deane, G. B., Stokes, M. D., DeMott, P. J., Aluwihare, L. I., Palenik, B. P., Azam, F. and Seinfeld, J. H.: Bringing the ocean into the laboratory to probe the chemical complexity of sea spray aerosol, Proceedings of the National Academy of Sciences, 110, 7550-7555, 2013.

Prenni, A. J., Tobo, Y., Garcia, E., DeMott, P. J., Huffman, J. A., McCluskey, C. S., Kreidenweis, S. M., Prenni, J. E., Pöhlker, C. and Pöschl, U.: The impact of rain on ice nuclei populations at a forested site in Colorado, Geophysical Research Letters, 40, 227-231, 10.1029/2012gl053953, 2013.

Pringle, A., Patek, S. N., Fischer, M., Stolze, J. and Money, N. P.: The captured launch of a ballistospore, Mycologia, 97, 866-871, 10.3852/mycologia.97.4.866, 2005.

Pummer, B. G., Bauer, H., Bernardi, J., Bleicher, S. and Grothe, H.: Suspendable macromolecules are responsible for ice nucleation activity of birch and conifer pollen, Atmos. Chem. Phys., 12, 2541-2550, 10.5194/acp-12-2541-2012, 2012.

Robinson, N. H., Allan, J. D., Huffman, J. A., Kaye, P. H., Foot, V. E. and Gallagher, M.: Cluster analysis of WIBS single-particle bioaerosol data, Atmospheric Measurement Techniques, 6, 337-347, 10.5194/amt-6-337-2013, 2013.

Rockett, T. R. and Kramer, C. L.: Periodicity and Total Spore Production by Lignicolous basidiomycetes, Mycologia, 66, 817-829, 1974.

Sands, D. C., Langhans, V. E., Scharen, A. L. and de Smet, G.: The association between bacteria and rain and possible resultant meteorological implications, Journal of the Hungarian Meteorological Service, 86, 148-152, 1982.

Schumacher, C. J., Pöhlker, C., Aalto, P., Hiltunen, V., Petäjä, T., Kulmala, M., Pöschl, U. and Huffman, J. A.: Seasonal cycles of fluorescent biological aerosol particles in boreal and semi-arid forests of Finland and Colorado, Atmos. Chem. Phys., 13, 11987-12001, 10.5194/acp-13-11987-2013, 2013.

Sesartic, A., Lohmann, U. and Storelvmo, T.: Modelling the impact of fungal spore ice nuclei on clouds and precipitation, Environ. Res. Lett., 8, 014029, 10.1088/1748-9326/8/1/014029, 2013.

Setlow, B. and Setlow, P.: Levels of Oxidized and Reduced Pyridine Nucleotides in Dormant Spores and During Growth, Sporulation, and Spore Germination of Bacillus megaterium, J. Bacteriol., 129, 857-865, 1977.

Shiraiwa, M., Selzle, K. and Poeschl, U.: Hazardous components and health effects of atmospheric aerosol particles: reactive oxygen species, soot, polycyclic aromatic compounds and allergenic proteins, Free Radical Research, 46, 927-939, 10.3109/10715762.2012.663084, 2012.

Sivaprakasam, V., Huston, A. L., Scotto, C. and Eversole, J. D.: Multiple UV wavelength excitation and fluorescence of bioaerosols, Optics Express, 12, 4457-4466, 2004.

983 Sivaprakasam, V., Lin, H.-B., Huston, A. L. and Eversole, J. D.: Spectral
984 characterization of biological aerosol particles using two-wavelength excited laser-
985 induced fluorescence and elastic scattering measurements, Optics Express, 19, 6191-
986 6208, 2011.

987 Stanley, W. R., Kaye, P. H., Foot, V. E., Barrington, S. J., Gallagher, M. and Gabey,
988 A.: Continuous bioaerosol monitoring in a tropical environment using a UV
989 fluorescence particle spectrometer, Atmospheric Science Letters, 12, 195-199,
990 10.1002/asl.310, 2011.

991 Sterling, M., C. Rogers and Levetin., E.: An evaluation of two methods used for
992 microscopic analysis of airborne fungal spore concentrations from the Burkard Spore
993 Trap., Aerobiologia, 15, 9-18, 1999.

994 Tanke, H. J., van Oostveldt, P. and van Duijn, P.: A parameter for the distribution of
995 fluorophores in cells derived from measurements of inner filter effect and
996 reabsorption phenomenon, Cytometry, 2, 359-369, 10.1002/cyto.990020602, 1982.

997 Toprak, E. and Schnaiter, M.: Fluorescent biological aerosol particles measured with
998 the Waveband Integrated Bioaerosol Sensor WIBS-4: laboratory tests combined with
999 a one year field study, Atmospheric Chemistry and Physics, 13, 225-243,
1000 10.5194/acp-13-225-2013, 2013.

1001 Womack, A. M., Bohannan, B. J. M. and Green, J. L.: Biodiversity and biogeography
1002 of the atmosphere, Philosophical Transactions of the Royal Society B: Biological
1003 Sciences, 365, 3645-3653, 10.1098/rstb.2010.0283, 2010.

1004 Xu, Z., Wu, Y., Shen, F., Chen, Q., Tan, M. and Yao, M.: Bioaerosol Science,
1005 Technology, and Engineering: Past, Present, and Future, Aerosol Sci. Technol., 45,
1006 1337-1349, 10.1080/02786826.2011.593591, 2011.

1007

1008

1009 **Table 1.** A comparison between instrumental parameters used during the study for the
1010 UV-APS and WIBS-4 techniques.

	UV-APS (TSI Model no. 3314)	**WIBS (Univ. Hertfordshire Model no. 4)**
Summary of measurement capabilities	particle size, intrinsic particle fluorescence (1 channel), particle side-scatter light intensity	particle size, intrinsic particle fluorescence (3 channels), particle asymmetry
Aerosol sample flow rate	1.0 L min^{-1}	0.23 L min^{-1}
Sampling Time	User-defined binning (5-min here)	Individual particle detection (post-binned to 5-min)
Sizing Method	Aerodynamic Diameter (D_a)	Optical Diameter (D_o)
Size resolution	52 channels selected	52 channels selected (only 45 channels used due to max D_o ~13 µm)
Particle Size Range	D_a: ~0.5 to ~20 µm	D_o: ~0.5 µm to ~13 µm
Excitation source	355 nm via UV laser (Nd:YAG)	280 nm and 370 nm via Xenon flash-tubes with blocking filters
Fluorescence	λ_{ex} = 355 nm λ_{em} = 420 – 580 nm	FL 1: λ_{ex} = 280 nm, λ_{em} = 310 – 400 nm
		FL 2: λ_{ex} = 280 nm, λ_{em} = 420 – 650 nm
		FL 3: λ_{ex} = 370 nm, λ_{em} = 420 – 650 nm
Particle Asymmetry	n/a	A_F via side-scatter intensity in four quadrants (A_F = 0, sphere; A_F >> 0, high aspect ratio fibre)

1011
1012

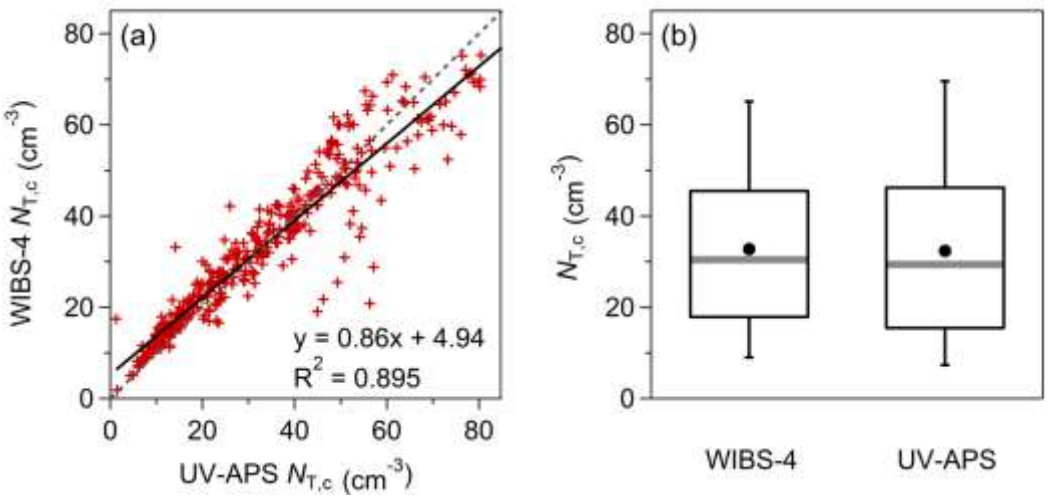

Figure 1. Comparison of concentrations of total coarse particles (D > 1 µm) over the entire ~1 month measurement period. Red symbols (a) show 5-minute data points, and solid black line shows linear fit (not weighted). Dashed line is 1:1 line. Statistical summary of $N_{T,c}$ shown as box-whisker plots (b). Black dots (mean), horizontal gray bar (median), boxes (25-75th percentile), vertical bars (5-9th percentile).

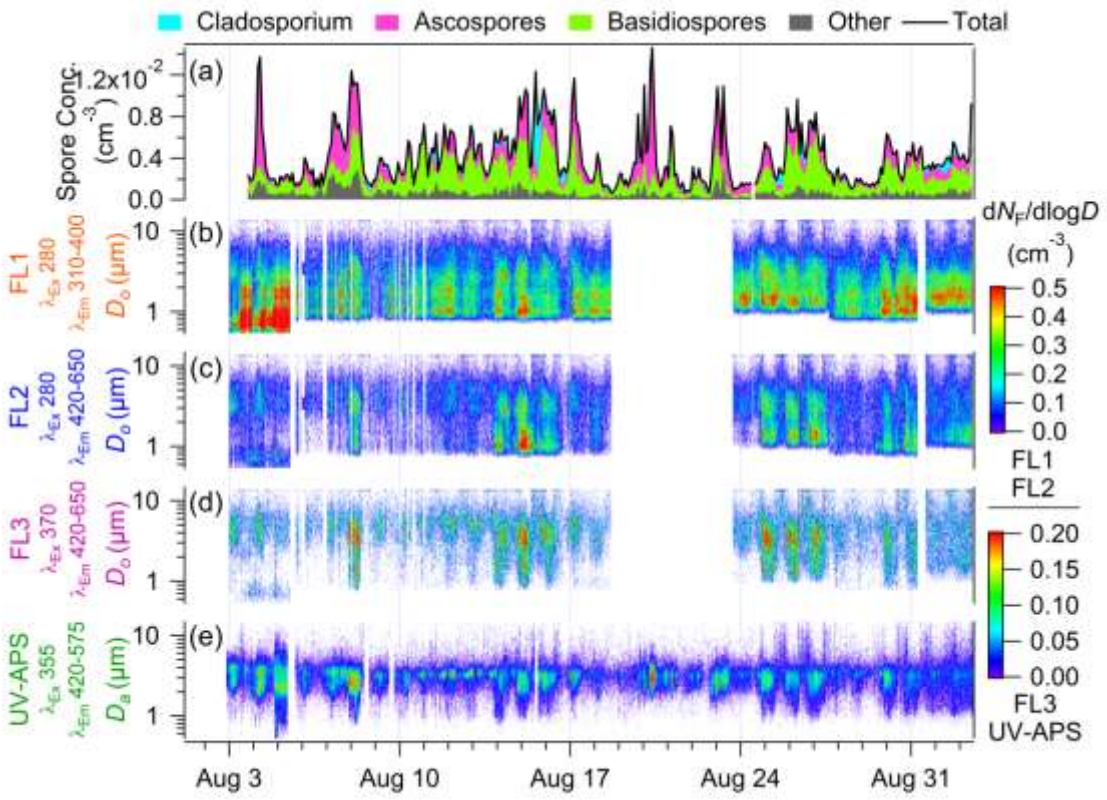

Figure 2. Campaign overview time series. Selected biological particles identified by Sporewatch technique (a). Size-resolved measurements of fluorescent particles as determined by: WIBS FL1 (b), FL2 (c), and FL3 (d) channels, and UV-APS (e). Color scale for image plots (b-e) shown as $dN_F/d\log D$ (cm^{-3}) on right and is separated into FL1, FL2 (upper scale) and FL3, UVAPS (lower scale). Data reported for both WIBS-4 and UV-APS as 5-min averages and for Sporewatch as 2 hr averages.

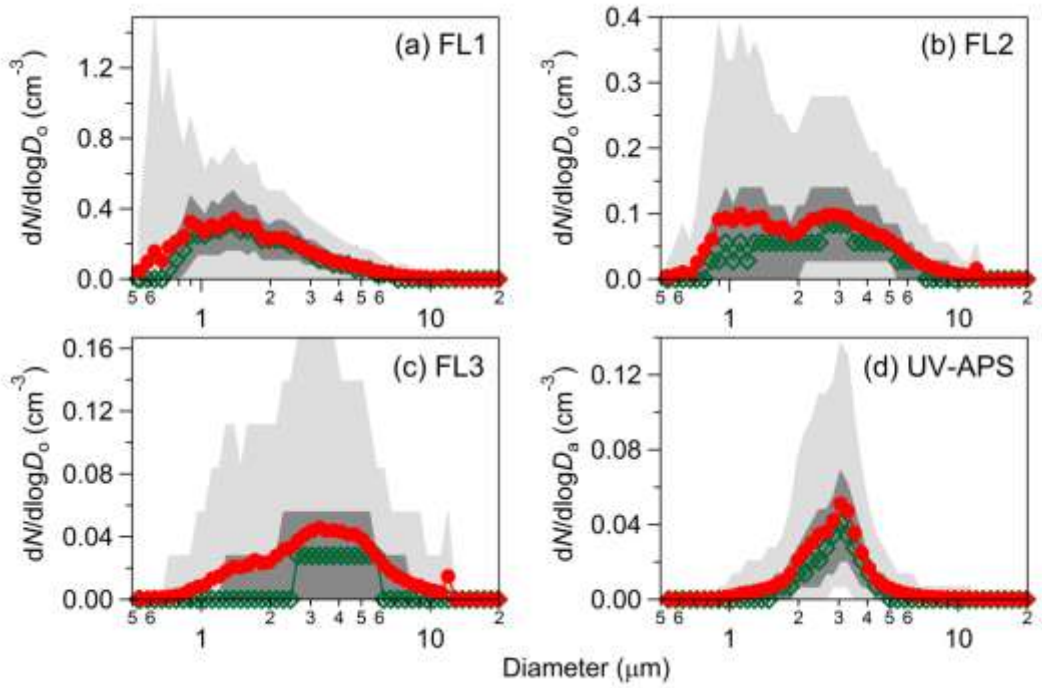

Figure 3. Average FBAP number size distributions measured by WIBS-4 for (a) FL1, (b) FL2 (c) FL3 and (d) UV-APS for the entire sampling period. Red traces show mean values, green traces show median, dark gray areas show 25-75th percentile, and light gray areas show 5-95th percentiles. Vertical scacle is different in each panel.

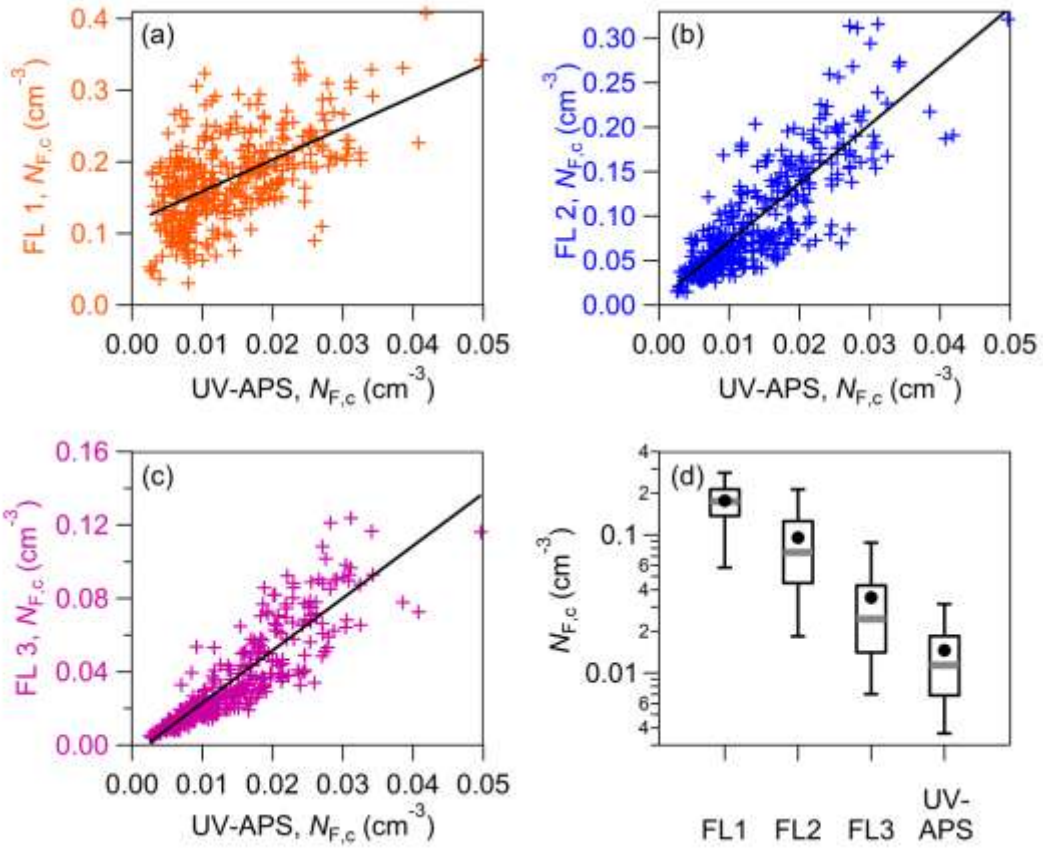

Figure 4. Comparison of coarse (> 1 µm) fluorescent particle number ($N_{F,c}$) between individual WIBS channels and UV-APS shown for entire measurement period. Coloured crosses show individual 5-minute data (a-c), and black diagonal lines show un-weighted linear fits. Correlation coefficients are: FL1, R^2 0.34 (a); FL2, R^2 0.68 (b); FL3, R^2 0.78 (c). Statistical overview of all data shown for each channel as box-whisker plots (d); black dot mean, horizontal gray bar median, black box 25-75th percentile, vertical bars 5-95th percentiles. Vertical scales are different in each correlation plot (a-c).

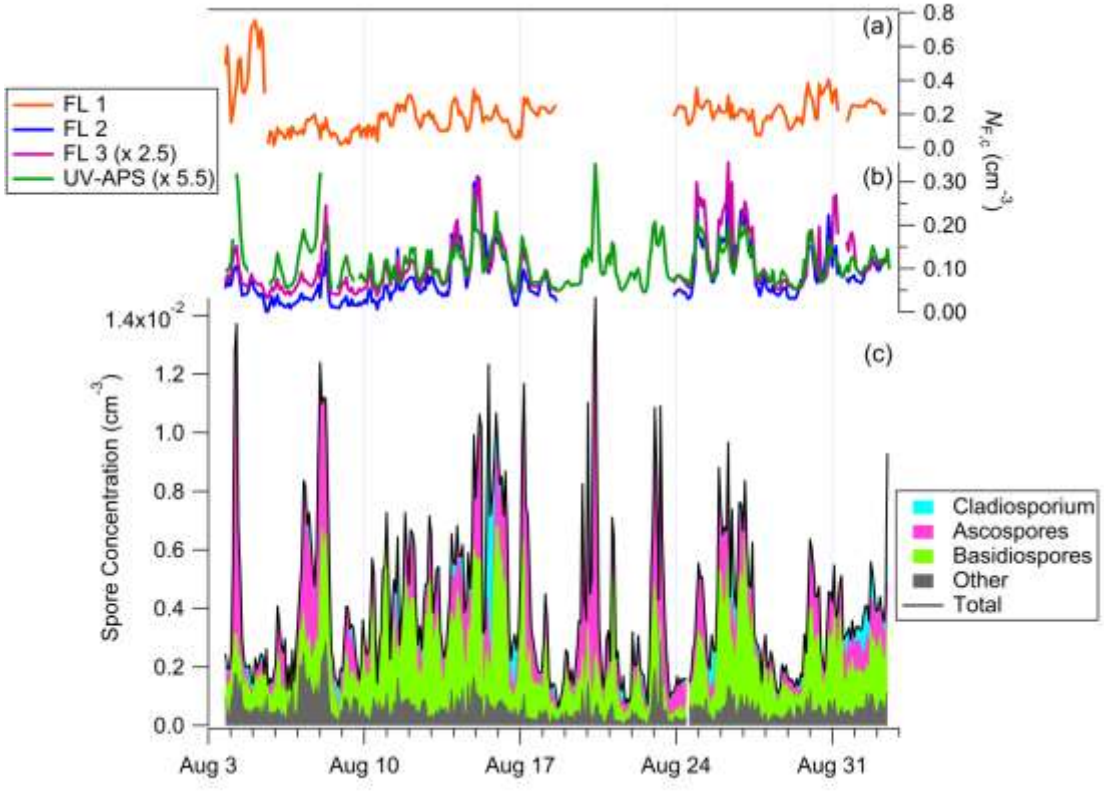

Figure 5. Temporal trends observed for coarse fluorescent particles (a-b) and spores sampled by Sporewatch (c). WIBS FL1 $N_{F,c}$ plotted alone (a), WIBS FL2, FL3, and UV-APS $N_{F,c}$ traces plotted together (b). Scaler value for FL3 and UV-APS traces shown in legend, showing that these traces have been multiplied by the value to show on one axis. All three vertical axes have different scales.

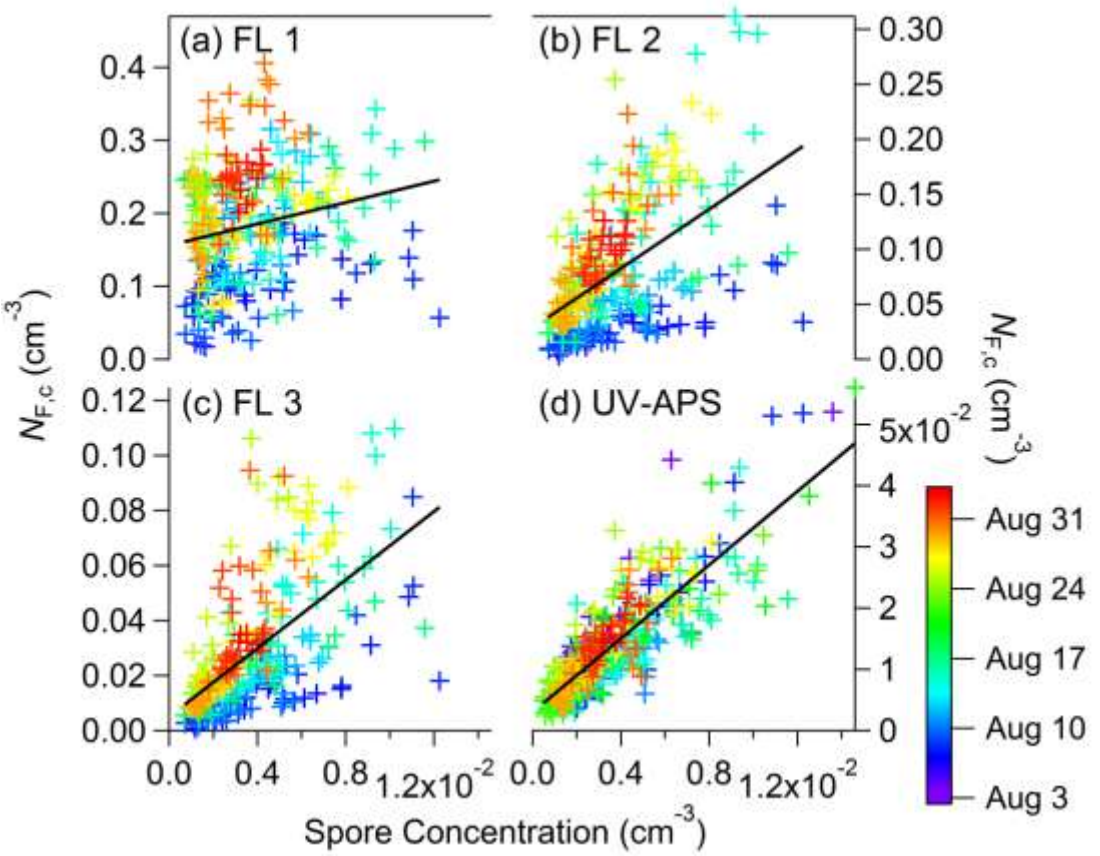

Figure 6. Demonstrated relationship of $N_{F,C}$ determined by the real-time instruments versus a sum of a subset of spores collected by the Sporewatch impactor. Spores here include: ascospores, basidiospores, and *Ganoderma spp*, which relate approx. 88% of total spore concentration (remaining percentage *Cladosporium spp.*). Crosses represent 2 hr measurement points, coloured by sampling date. Black lines represent un-weighted linear fits, with coefficients as follows: (a) FL1 (m = 7.67, R^2 = 0.052); (b) FL2 (m = 14.03, R^2 = 0.290); (c) FL3 (m = 6.47, R^2 = 0.380); (d) UV-APS (m = 3.00, R^2 = 0.710). All vertical axes have different scales.

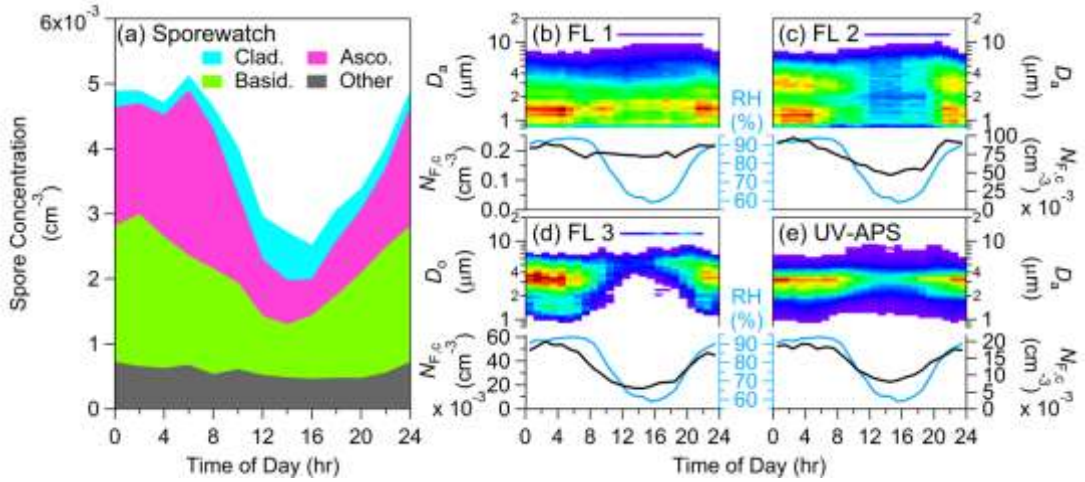

Figure 7. Diurnal plots of number concentrations from Sporewatch (a) and real-time fluorescence instruments (b-e) as median values for entire sampling period. Upper panel of WIBS and UV-APS plots (b-e) show size-resolved image, with colour scale qualitatively similar to Fig. 2 (warmer colours, higher concentration). Lower panel of the same plots show integrated fluorescent particle number ($N_{F,c}$; D > 1 µm) as black trace and relative humidity as blue trace. Vertical scale on $N_{F,c}$ axes not consistent. $N_{F,c}$ scale for (c-e) shown expanded by 10^3.

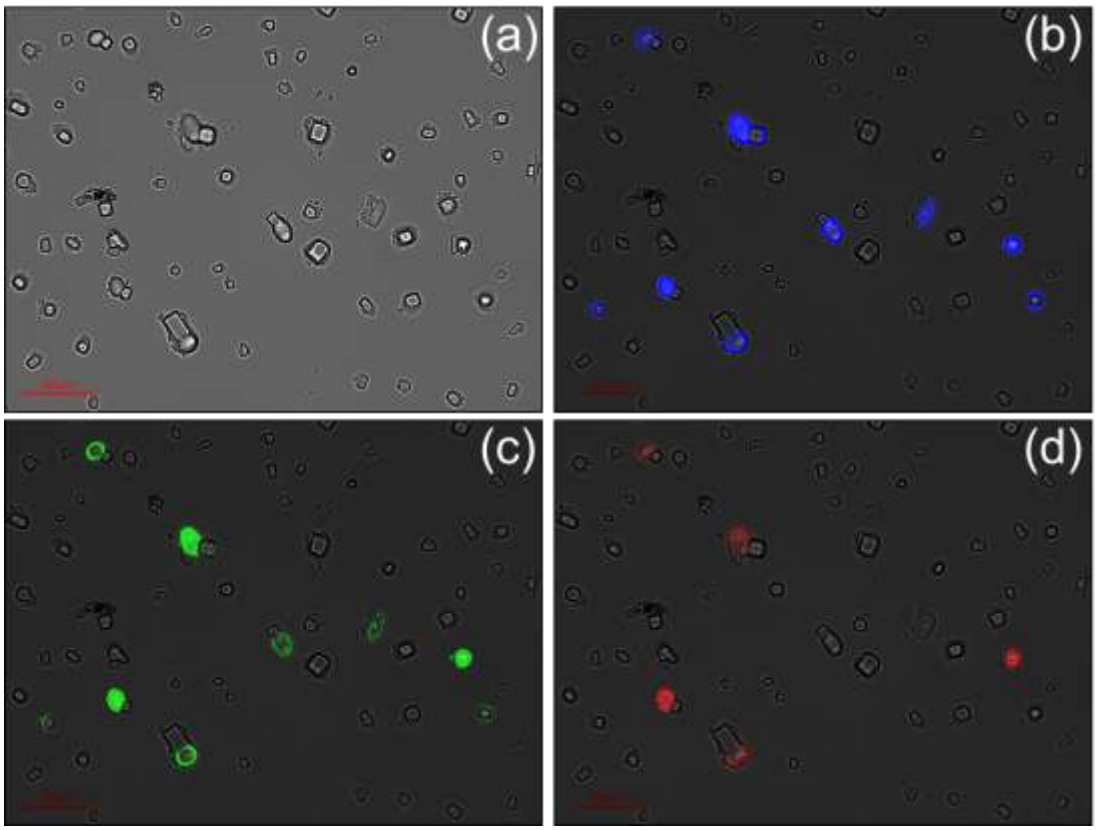

Figure 8. Fluorescence microscopy images of ambient aerosols collected on MOUDI stage 5 (size range, *D* 1.0 – 1.8 μm) on 25 August, 03:00 – 07:00 (LT). Illumination source: (a) bright field, (b) λ_{ex} = 340 – 380nm, λ_{em} = 435 – 485, (c) λ_{ex} = 465 – 495nm, λ_{em} = 510 – 560, (d) λ_{ex} = 540 – 580nm, λ_{em} = 600 – 660. Magnification × 1000.